



THE UNIVERSITY *of* EDINBURGH

Edinburgh Research Explorer

Quantifying self-heating ignition of biochar as a function of feedstock and the pyrolysis reactor temperature

Citation for published version:

Restuccia, F, Masek, O, Hadden, R & Rein, G 2019, 'Quantifying self-heating ignition of biochar as a function of feedstock and the pyrolysis reactor temperature', *Fuel*. <https://doi.org/10.1016/j.fuel.2018.08.141>

Digital Object Identifier (DOI):

[10.1016/j.fuel.2018.08.141](https://doi.org/10.1016/j.fuel.2018.08.141)

Link:

[Link to publication record in Edinburgh Research Explorer](#)

Document Version:

Publisher's PDF, also known as Version of record

Published In:

Fuel

General rights

Copyright for the publications made accessible via the Edinburgh Research Explorer is retained by the author(s) and / or other copyright owners and it is a condition of accessing these publications that users recognise and abide by the legal requirements associated with these rights.

Take down policy

The University of Edinburgh has made every reasonable effort to ensure that Edinburgh Research Explorer content complies with UK legislation. If you believe that the public display of this file breaches copyright please contact openaccess@ed.ac.uk providing details, and we will remove access to the work immediately and investigate your claim.





Full Length Article

Quantifying self-heating ignition of biochar as a function of feedstock and the pyrolysis reactor temperature

Francesco Restuccia^a, Ondřej Mašek^b, Rory M. Hadden^c, Guillermo Rein^{a,*}

^a Department of Mechanical Engineering, Imperial College London, United Kingdom

^b School of Geosciences, University of Edinburgh, United Kingdom

^c School of Engineering, University of Edinburgh, United Kingdom

ARTICLE INFO

Keywords:

Self-heating

Biochar

Reactivity

Fire safety

ABSTRACT

Biochar is produced from biomass through pyrolysis in a reactor under controlled conditions. Different feedstock and reactor temperatures produce materials with different physical and chemical properties. Because biomass, biochar and torrefied biomass are reactive porous media and can undergo self-heating, there is a fire hazard associated to their production, transport, and storage. This hazard needs to be tackled in biomass industries like power generation, where self-heating of biomass can cause significant problems, like the 2012 fire at Tilbury Power Plant (UK). Using basket experiments inside a thermostatically controlled laboratory oven, augmented with thermogravimetry and conductivity measurements, we experimentally study the ignition conditions of pellets and biochar made of softwood, wheat and rice husk. For softwood, we also study biochar produced at different reactor temperatures ranging from 350 to 800 °C. In total, 173 experiments were conducted with 1036 h of oven run time. By investigating the self-heating behaviour of these samples via the Frank-Kamenetskii theory, we quantify and upscale for the first time the reactivity of biochar as a function of feedstock and also of the reactor temperature. The results show that in order from higher to lower tendency to self-heating, the rank is softwood, wheat and rice husk. The reactivity of the softwood is not a monotonic function of pyrolysis reactor temperature but that biochar is most prone to self-heating when produced at 450 °C. Reactivity decreases at higher reactor temperatures, and at 600 °C the biochar is less reactive than the original feedstock. This work improves the fundamental understanding of the fire hazard posed by biomass self-heating, providing insights necessary for successful and safer biomass industries.

1. Introduction

Biomass, plant-based materials collected by humans which are not used for food or animal feed, have historically been waste material or used as a form of energy source, especially in the form of wood. So, over the past number of years, biomass has become an important part of the fuel mix for fossil fuel power plants, and its use is projected to grow significantly [1].

Torrefied biomass, a product of biomass pyrolysis, is a possible replacement for coal, as it could integrate into existing coal power plants, enabling power plants to generate clean energy without an expensive conversion process [2]. At the same time biochar, charcoal produced from the pyrolysis of biomass, is being used for soil amendment for very acidic soils. Furthermore, carbon remains sequestered in biochar for centuries, so sustainable biochar production allows for atmospheric carbon sequestration. However, there are fire safety issues associated

with both biomass and biochar. Both biochar and torrefied biomass are solid biomass pyrolysis products. They are derived from biomass through pyrolysis in a reactor under controlled conditions. Different reactor temperatures produce different pyrolyzed biomass, leading to materials with different properties and reactivities [3]. For reactor temperatures below 350 °C, this solid material is called torrefied biomass. For temperatures greater than 350 °C, this solid material is called biochar [3].

Reactive porous media such as wood, biomass, biochar, organic soils and coal have small free spaces (i.e. pores, voids) embedded in the solid together with a presence of a carbon-rich component [4]. This allows the media to be permeable to air and greatly increases its surface area per unit volume, making the organic media reactive by allowing heterogeneous oxidation reactions to take place when oxygen is present [5]. Such reactive porous media have been shown to undergo self-heating [6,7]. Self-heating is the tendency of certain porous fuels to

* Corresponding author.

E-mail address: g.rein@imperial.ac.uk (G. Rein).

<https://doi.org/10.1016/j.fuel.2018.08.141>

Received 25 January 2018; Received in revised form 20 April 2018; Accepted 30 August 2018

0016-2361/ © 2018 The Authors. Published by Elsevier Ltd. This is an open access article under the CC BY license (<http://creativecommons.org/licenses/by/4.0/>).

undergo spontaneous exothermic reactions in oxidative atmospheres at low temperatures [7]. In biomass, this process typically starts by exothermic biological reactions, which can occur at temperatures up to 70 °C [8]. The further exothermicity is then dominated by slow exothermic oxidation at low temperatures, but the reaction alone is insufficient to raise the material temperature. The temperature rise is determined by the balance between the rate of heat generation and the rate of heat losses [9]. These exothermic reactions can lead to ignition, leading to smouldering or flaming fires. The more reactive the material, the more prone it is to self-heat. Fire initiated by self-heating ignition is a well-known problem for many porous reactive media, and has been reported and studied for materials such as chemically activated carbon, sawdust, wood, coal, organic soils, biomass and shale [6,10–13]. Some work has been carried out on the self-heating ignition properties of biomass utilising thermogravimetric analysis (TGA) on a variety of materials such as poplar wood and wheat straw [14–17]. TGA is very useful for determining kinetics, but is not sufficient to characterise self-heating, as the assumption for TGA measurements is that the sample can be considered 0D. In reality, self-heating requires understanding of the heat distribution in space as self-heating will occur at the centre of a sample. Therefore analysis is required to be able to analyse the bulk behaviour of biomass self-heating ignition. Some of this work is present in literature: Garcia et al. [18] carried out some of these bulk property studies on the self-heating ignition properties of biomass dust, and its propensity to ignite in storage conditions where oxygen is present and the environmental temperature is elevated enough. Jones et al. [19] studied self-heating ignition properties using TGA coupled with basket experiments for a variety of biomass feedstock including olive residue, sugars, and sunflower husks. Some work was also carried out to predict self-heating ignition of biomass by analysing emission products [20]. This work focuses on quantifying the relationship between characteristic material properties of biochar, namely pyrolysis temperature and physical properties of the char, on the tendency of the material to ignite due to self-heating.

2. Theory

2.1. Biochar reactivity

In-depth studies of biomass pyrolysis have been previously carried out in literature to determine the pyrolysis effect on the three major components of biomass: cellulose, hemicellulose and lignin [21,22]. They showed that at heating rates lower than 100 °C/min biomass decomposes first by hemicellulose decomposition, then cellulose decomposition and finally lignin which decomposes more slowly. Moisture evaporation will occur at temperatures below 110 °C. For the decomposition, hemicellulose was found to have most of its weight loss in the temperature range between 220 °C and 315 °C, cellulose in the temperature range between 315 °C and 400 °C, and lignin as a slower process with only 67% of its weight lost by 850 °C [21].

Biochar is defined as a porous carbonaceous solid produced by the thermochemical conversion of organic materials in the absence of oxygen. Because of its production temperatures above 350 °C, lignin is the main component of biochar produced from biomass. Biochar also contains aromatic-aliphatic organic compounds of complex structure which include residual volatiles, and ash. Biochar has a higher carbon density compared to the original biomass feedstock. Finally, there are voids in the biochar structure formed as pores (macro, meso and micropores), cracks and morphologies of cellular biomass origin making biochar a reactive porous structure [23]. This porous structure makes biochar prone to self-heating ignition.

2.2. Frank-Kamenetskii theory

The problem in self-heating ignition corresponds to the transient heat conduction equation. There are three main models that can be

used in analysing oxidation and self-heating reactions present in this heat transfer problem [24]. The first model is the Semenov model, which describes spontaneously-heating systems by assuming uniform temperature distributions, neglecting consumption of the reactant material and assuming that the chemical reaction follows a one-step Arrhenius temperature dependence. The second model is the Frank-Kamenetskii model, which builds on the Semenov model but incorporates heat conduction through the solid material due to the chemical heat release of the material, therefore does not assume uniform temperature profiles. The third available model is known as the Thomas model and it builds upon the Frank-Kamenetskii model by additionally considering the convective heat loss effects from the surface. All three models assume a single-step global reaction, constant thermal properties of the material, no reactant consumption and no restriction of oxidizer availability [7,25]. Therefore they only apply to materials for which a global one-step kinetic model provides a reasonable approximation to the actual chemical scheme of the material. The most used model for experimental work in the literature to investigate self-ignition properties of materials is the Frank-Kamenetskii theory of ignition criticality [6,7,12,26]. The reason for this is that a basket heating experimental technique was developed based on this theory which allows the determination of critical ambient temperatures for a given sample size for ignition. The theory can be used to extrapolate data from experimental measurements to predict the expected behaviour of very large stockpile sizes of that same material. The data and the analysis serve to quantify the risks in realistic conditions if the mechanism of heat generation is unchanged when extrapolating the results to larger sizes [7,26]. These models are very effective when used to predict critical temperature and critical size for ignition, but are not as effective when used to assess the time to ignition, as the models assume steady-state conditions and therefore make the time to ignition harder to quantify. The disadvantage of using Frank-Kamenetskii theory coupled with basket experiments is that it is a very time-intensive method and requires a lot of material, as many experiments have to be carried out. However, Frank-Kamenetskii theory coupled with the oven basket methodology has been shown to give the most robust results for scaling results of laboratory-scale experiments to larger size [7,26]. Therefore despite it requiring a large time and resource investment, this method was used to obtain robust results that can be utilised to study the widest range of length scales.

To carry out the analysis of experimental results, the Frank-Kamenetskii theory of ignition assumes that the material being studied is reactive and 1D, and that the heat release is from a 1-step exothermic reaction which contains numerous chemical and biological elemental reactions as described earlier. For organic materials such as biomass there are two main sources of heat generation that make up this global 1-step reaction, a chemical process at higher temperatures and a biological process at lower temperatures [27]. The biological process can range from temperatures under 20 °C to up to 70 °C and is usually caused by growths of psychrophilic, mesophilic and thermophilic micro-organisms [28]. The biological process will have a contributing effect at lower temperatures in raising the biomass temperature. However already from 40 °C chemical oxidation will start contributing to the heat generation and as the temperature increases it becomes the dominating heat generation process [28]. This global reaction is also assumed to have a high activation energy so that a steady-state solution exists [7,26].

To solve the transient heat conduction equation, Frank-Kamenetskii theory defines a dimensionless parameter δ (Eq. (1)),

$$\delta = \frac{QE_f L^2}{kRT_a^2} e^{-\frac{E}{RT_a}} \quad (1)$$

where E is the activation energy of the 1-step global oxidation reaction, k is the effective thermal conductivity of the sample, R the universal gas constant, T_a is the ambient temperature, L is the characteristic length of

the sample (for a cube basket the side length, and for an infinite slab the thickness), Q is the heat of reaction per fuel mass, and f is the value of the mass action law which relates the concentration of fuel and oxygen at the initial time to reaction rates, and is based on initial concentrations of fuel and oxygen [26]. Expressing the reaction rate as the Arrhenius law for dependence on temperature, the transient heat conduction equation is solved and the following dependence of critical sample size and ambient temperature is obtained, Eq. (2).

$$\ln\left(\frac{\delta_c T_{a,c}^2}{L^2}\right) = \ln\left(\frac{QEf}{Rk}\right) - \frac{E}{RT_{a,c}} \quad (2)$$

where δ_c is the critical value of the dimensionless parameter in Eq. (1) for which ignition occurs, which is a function of the geometrical shape of fuel; and $T_{a,c}$ is the critical (minimum) ambient temperature for which self-ignition occurs. This parameter can be considered analogous to the critical Damköhler number.

A solution to Eq. (2) satisfying the boundary condition at the surface $T = T_a$ only exists when the condition $\delta \leq \delta_c$ is satisfied. δ_c is a function of geometry which has been precisely calculated and can be found in the literature [6,10,26]. The experimental work carried out in this paper utilises cubic baskets, which have a critical value $\delta_c = 2.52$ [26]. The experimental setup, discussed in the next session, has symmetric boundary conditions, allowing the use of Frank-Kamenetskii theory as presented in this section to model the 3-dimensional physical problem as a 1-dimensional mathematical problem.

In addition to the conditions stated in the derivation of these equations, when carrying out basket experiments with environmental temperatures greater than 100 °C the effect of moisture cannot be accounted for as the thermostatically controlled ovens used for measurements are at temperatures greater than the boiling point of water. The effect of moisture content has been studied for biomass combustion [29]. However the effect of moisture content (MC) on self-heating ignition of reactive porous media has been shown to be complex [30]. At low MC an increase in moisture content increases the reactivity of the material, so the tendency for it to self-heat. At higher MC values the reactivity of the material decreases dramatically with moisture content [30]. For self-heating of coal, which has been studied extensively in the past, moisture content affects the type of radical sites formed in the porous material. At low MC, up to approximately 50% MC, the presence of moisture increases the self-heating process [31]. At higher MC and higher conductivity any non-tightly bound moisture, so excess moisture, takes up extra heat and slows down the release of heat from oxidation [31]. However this work will not consider the effect of moisture content as it is not derivable from self-heating basket experiments.

3. Materials and method

To carry out this experimental work on self-heating ignition of softwood biomass pellets and biochar, a series of biochars were produced in a bench-scale pyrolysis reactor at the UK biochar Research Centre at the University of Edinburgh. The reactor is a rotary-kiln pyrolysis reactor, with pyrolysis temperatures between 350 °C and 800 °C, following the experimental procedure presented in [32]. The biochars used for this experimental work were produced from a softwood pellet feedstock pyrolysed in a reactor at 350 °C, 400 °C, 450 °C, 550 °C, 600 °C, 700 °C and 800 °C. At reactor temperatures below 350 °C the product would not be biochar so temperatures below that threshold were not considered. The softwood feedstock are puffin pellets, premium grade, and are made up of a mix of pine and spruce [32]. The mean kiln residence time for the samples was 12 min, and details about the pyrolysis process are found in [32]. The samples are presented in Fig. 1, and show different physical properties in terms of diameter, average length, and bulk density. A summary of these characteristics is presented in Table 1. As can be seen in the table the density and

diameter of the pellets reduces with increasing pyrolysis temperature as more of the softwood pyrolyses, but for pyrolysis above temperatures of 450 °C the bulk density and diameter of the particle does not change as significantly as up to 450 °C. This was also seen in Fig. 1 visually as the particles become much darker and smaller. Elemental analysis of the biochars and biomass is presented in Table 2, where it can be seen that the percentage of mass of the biochar is increasingly carbon with increasing reactor temperature. This agrees with results from literature [33]. Water, ash and carbon in dry ash free basis (Cdaf) for the softwood and its biochar are calculated using the TGA data presented in 4.2. The carbon in dry ash free basis is calculated according to the BSI standard EN 15296:2011 [34]. Results are presented in Table 3, where it can be seen that for all the biochars, carbon content is above 61%, and biochars produced at reactor temperatures above 700 °C are purely carbon apart from water and ash.

The laboratory setup to determine the minimum critical ambient temperature for self-heating $T_{a,c}$ that leads to self-ignition was constructed following a similar procedure to the British Standards EN 15188:2007 and has been previously used in the authors' work [11,12]. Fig. 2 shows the overall experimental setup, with the three basket sizes filled with softwood feedstock pellets as sample representations of a typical basket setup. The pellets were packed into cubic shaped wire mesh baskets of three different sizes to ensure sufficient data could be measured to assess if the assumption of Arrhenius reactions necessary to adopt Frank-Kamenetskii theory could be applied. As in previous work, cube shaped baskets were selected as it is the shape most easily adaptable to increasing basket size in a rectangular oven without making the larger samples approach the oven walls. The baskets were made of 0.5 mm diameter wire mesh with volumes of 131, 442 and 1049 cm³. These basket sizes give us the largest variation in size possible with both the oven size and amount of biochar available for the experiments. These baskets ensure a good range of sizes for the largest possible temperature range given at the laboratory scale, between 90 °C and 200 °C for these softwood samples. As the basket size increases the critical ignition temperature reduces because the ratio of heat losses to the environment to heat generated by chemical reactions decreases [10]; therefore, the larger the baskets in the experimental setup, the more accurate the predictions that can be extracted from the results when upscaling to large stockpile sizes. Each basket filled with pellets was placed in the centre of a laboratory oven with forced air circulation to prevent temperature stratification and provide good oxygen supply. The oven was initially preheated to a given uniform ambient temperature T_a . In order to limit the influence of the forced flow, a large mesh cage was placed around the sample. The temperature inside the sample was monitored using two thermocouples placed at the centre of the sample 0.5 cm apart. Based on the standard, only one thermocouple is needed, so the second one provides redundancy. Oven temperature was also measured by a thermocouple placed several centimetres away from the basket, inside the mesh cage, in the vertical middle plane of the oven.

In total, 92 experiments were carried out for softwood with 567 h of oven run time. A summary of the experiments carried out is presented in Table 4. If the softwood failed to reach ignition the experiment was repeated with a fresh sample at a higher temperature. If the softwood reached ignition, then the experiment was repeated with a fresh sample at a lower temperature. The experiments were carried out until $T_{a,c}$ for ignition was located within ± 4 °C for each tested biomass. A minimum of two experiments was conducted at each basket size for each softwood sample.

In addition to the basket experiments, thermogravimetric analysis was conducted for each sample to provide information on the reaction kinetics of each sample at the microscale. Furthermore the conductivity of the softwood feedstocks and each biochar produced were measured for a range of temperatures between 65 °C and 165 °C. This was carried out to provide more data on the physical properties of the samples, so as to be able to extract more data from the self-heating basket

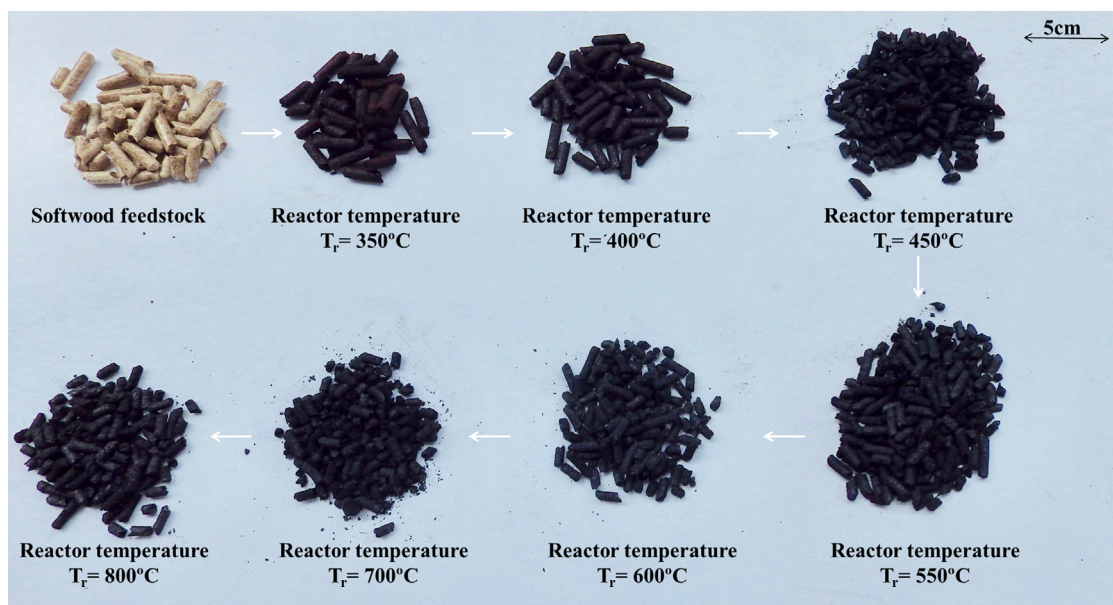


Fig. 1. Softwood samples used, with feedstock and various biochars produced in pyrolysis reactors at temperatures ranging from 350 °C to 800 °C.

Table 1

Physical properties of softwood biomass and biochar pellets produced at various reactor temperatures used for experiments. In parenthesis are ranges of lengths of pellets.

Physical properties	Density (kg/m ³)	Pellet length (mm)	Pellet diameter (mm)
Softwood feedstock	531	22 (19,25)	5.8
Produced at $T_r = 350$ °C	400	22 (19,25)	5.6
Produced at $T_r = 400$ °C	396	19 (16,22)	5.4
Produced at $T_r = 450$ °C	295	18 (15,21)	4.3
Produced at $T_r = 550$ °C	289	18 (15,21)	4.1
Produced at $T_r = 600$ °C	284	14 (12,16)	4.2
Produced at $T_r = 700$ °C	274	14 (12,16)	4.3
Produced at $T_r = 800$ °C	255	14 (12,16)	4.2

Table 2

Elemental analysis of the biomass and biochars produced at various reactor temperatures.

Element weight %	C	H	N
Softwood feedstock	45.8	6.4	< 0.3
Produced at $T_r = 350$ °C	58.8	5.4	< 0.3
Produced at $T_r = 400$ °C	58.7	5.6	< 0.3
Produced at $T_r = 450$ °C	76.8	3.8	< 0.3
Produced at $T_r = 550$ °C	82.3	3.2	< 0.3
Produced at $T_r = 600$ °C	84.0	2.8	< 0.3
Produced at $T_r = 700$ °C	86.3	2.6	< 0.3
Produced at $T_r = 800$ °C	89.6	1.7	0.4

Table 3

Water, ash and carbon in dry ash free basis (Cdaf) for the biomass and biochars calculated using the TGA data presented in Section 4.2.

Element	Water weight %	Ash	Cdaf
Softwood feedstock	5.5	0.9	48.9
Produced at $T_r = 350$ °C	4.2	2.7	63.1
Produced at $T_r = 400$ °C	2.3	1.7	61.1
Produced at $T_r = 450$ °C	4.2	1.8	81.6
Produced at $T_r = 550$ °C	3.8	3.0	88.3
Produced at $T_r = 600$ °C	4.0	3.2	90.5
Produced at $T_r = 700$ °C	4.6	9.0	99.9
Produced at $T_r = 800$ °C	3.6	6.6	99.8

experiments.

4. Results

4.1. Basket experiment measurements

Minimum ignition temperature, the lowest oven temperature required for ignition, was found for each basket for each sample type and is shown in Fig. 3.

As can be noted the lowest ignition temperature occurs for softwood biochar pyrolysed in a reactor at 450 °C. As mentioned in Section 2, biomass pyrolysis above 400 °C leaves mainly lignin in the biochar [21]. This can explain the increase in reactivity and proneness to self-heating ignition around the temperature of 450 °C reactor temperature because most of the cellulose and hemicellulose will have decomposed, leaving behind char and lignin. As reactor temperature further increases then the lignin also begins to decompose and we are left with less reactive carbon in the biochar. However the density and dimensions of the biochar pellets do not have significant changes above this temperature as shown in Table 1 and therefore there is less reactive material in the bulk system and the self-heating tendency decreases. For the explored basket sizes, for reactor temperatures above 600 °C the biochar becomes less prone to self-heating than the original softwood feedstock. These results show that the lowest ignition temperature for softwood biochar is not a monotonic function of the reactor temperature. In fact, after a gradual increase in reactivity with softwood produced at reactor temperatures of 350 °C and 400 °C there is a significant increase in reactivity for reactor temperatures of 450 °C, and then again a sharp decrease in reactivity for reactor temperatures above 550 °C. This result demonstrates that there is a very narrow range of reactor temperatures which produce softwood char that is far more reactive than any char produced at the rest of the reactor temperatures, and that maximum in reactivity lies at reactor temperature of 450 °C.

Plotting the minimum ignition temperature for one basket size (10.16 cm length basket) for all the biochars with respect to the carbon dry free ash allows a comparison of the effect of total carbon content with the critical ignition temperature and is done in Fig. 4. The results show that the peak at 450 °C is not solely caused by the carbon content, as the V shape seen in Fig. 3 is also clearly present in this plot.

Conductivity was measured experimentally using a guarded heat flow meter at various temperatures, and was shown to be linear

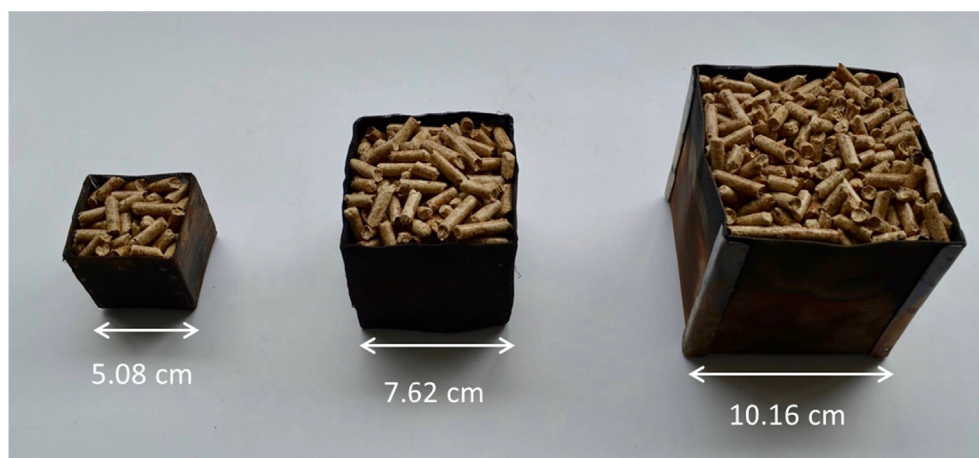


Fig. 2. Experimental setup for studying self-heating of a biomass sample placed at the centre of the thermostatically controlled oven using meshed experiment baskets filled with softwood feedstock.

Table 4

Number of experiments carried out for each type of softwood biochar and basket sizes.

Pellet type	Basket length l (cm)		
	5.1	7.6	10.2
Softwood feedstock	4	4	3
Produced at $T_r = 350^\circ\text{C}$	3	3	2
Produced at $T_r = 400^\circ\text{C}$	9	2	3
Produced at $T_r = 450^\circ\text{C}$	9	3	2
Produced at $T_r = 550^\circ\text{C}$	4	3	2
Produced at $T_r = 600^\circ\text{C}$	5	3	3
Produced at $T_r = 700^\circ\text{C}$	8	3	3
Produced at $T_r = 800^\circ\text{C}$	5	3	3

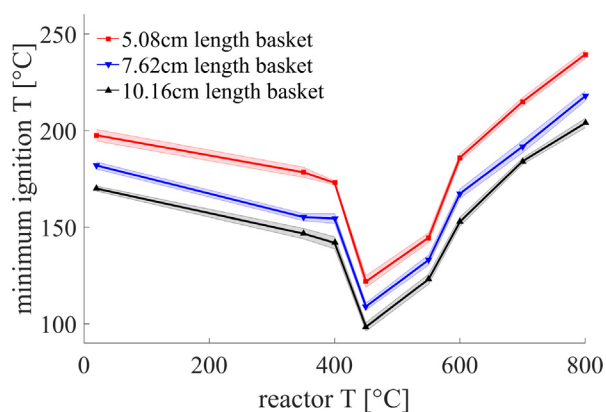


Fig. 3. Minimum ignition temperature for softwood feedstock and biochar between 350°C and 800°C for three basket sizes. Experimental error is estimated based on temperature error bounds on each individual set of experiments.

between 65 and 165°C . The most conductive of the softwood was the feedstock. The lowest thermal conductivity was found to be for softwood produced at reactor temperatures of 450°C . The percentage difference in thermal conductivity between the softwood produced at reactor temperatures of 450°C and the softwood feedstock, so between least and most reactive, was 27%. The lower conductivity of the 450°C biochar helps to further explain why this particular softwood biochar is most prone to self-heating, as the material acts as a good insulator, preserving the heat produced from the exothermic reactions within the centre of the sample and reducing the amount of cooling to the ambient. The summary of the conductivity measurements is presented in

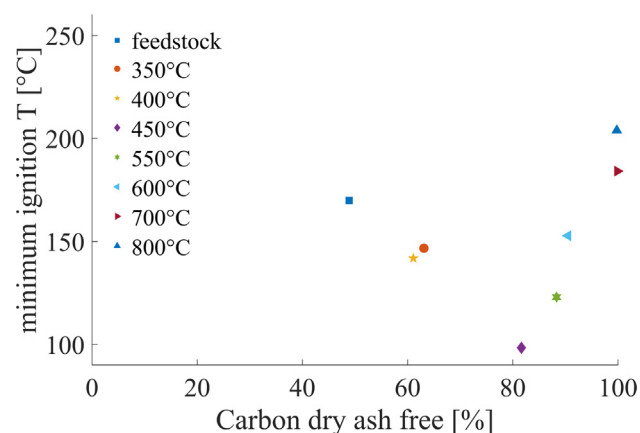


Fig. 4. Minimum ignition temperature for softwood feedstock and biochar between 350°C and 800°C for a fixed basket size plotted vs carbon dry ash free.

Table 5

Thermal conductivity measurements for the biomass samples conducted at 3 temperatures, with resulting fit equation. The R^2 values of the linear fits through these points is included.

k for biomass type	65°C (W/mK)	115°C (W/mK)	165°C (W/mK)	R^2 (–)
Softwood feedstock	0.1107	0.1228	0.1436	0.977
Produced at $T_r = 350^\circ\text{C}$	0.0936	0.1060	0.1147	0.990
Produced at $T_r = 400^\circ\text{C}$	0.1030	0.1060	0.1145	0.933
Produced at $T_r = 450^\circ\text{C}$	0.0807	0.0893	0.1004	0.995
Produced at $T_r = 550^\circ\text{C}$	0.0904	0.0917	0.0940	0.976
Produced at $T_r = 600^\circ\text{C}$	0.0903	0.1004	0.1055	0.964
Produced at $T_r = 700^\circ\text{C}$	0.0853	0.0919	0.0974	0.997
Produced at $T_r = 800^\circ\text{C}$	0.1027	0.1139	0.1192	0.960

Table 5.

To use Frank-Kamenetskii theory of criticality to extract a one-step kinetic model and thermal parameters from the basket experiments the data was used to make a $\ln(\delta_c T_{a,c}/L^2)$ vs $1/T_{a,c}$ plot (Fig. 5). In this plot, the slope of the straight line corresponds to $-E/R$. If the plot of $\ln(\delta_c T_{a,c}^2/L^2)$ against $1/T_{a,c}$ (Eq. (2)) is a straight line, it validates the Frank-Kamenetskii theory. As seen in Table 6, $R^2 > 0.975$ for all tested softwood samples, confirming the linearity of the slopes and therefore the validity of the Frank-Kamenetskii theory and 1-step global reactions assumption. Taking slopes in Fig. 5 gives the effective activation energies for the biomass. The y-intercept of these lines allows the

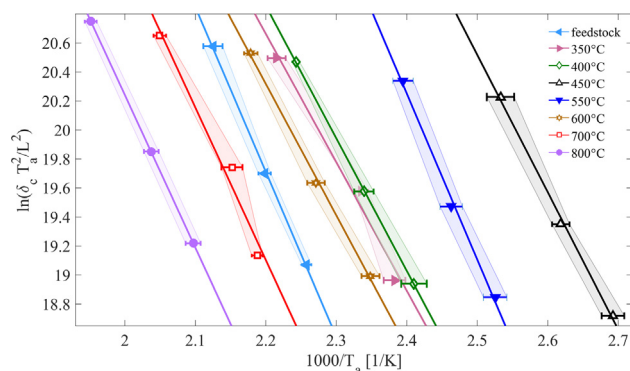


Fig. 5. Frank-Kamenetskii plot for softwood feedstock and biochar between 350 °C and 800 °C. Experimental error is estimated based on error bounds on each individual set of experiments. The linear fits all have $R^2 > 0.975$ (Table 6).

Table 6

Effective activation energy E , pre-exponential factor Qf , conductivity k extracted from Frank-Kamenetskii plot (Fig. 7) calculated using Eq. (2). The R^2 values of the linear fits used to calculate these is included.

Biomass type	E (kJ/mol)	k (W/mK)	Qf (W/m ³)	R^2 (–)
Softwood feedstock	94.52	0.1228	$2.86 \cdot 10^{14}$	0.999
Produced at $T_r = 350$ °C	73.65	0.1060	$3.28 \cdot 10^{12}$	0.982
Produced at $T_r = 400$ °C	76.01	0.1060	$7.19 \cdot 10^{12}$	1.000
Produced at $T_r = 450$ °C	78.76	0.0893	$1.48 \cdot 10^{14}$	0.997
Produced at $T_r = 550$ °C	95.18	0.0917	$4.27 \cdot 10^{15}$	0.996
Produced at $T_r = 600$ °C	75.37	0.1004	$3.38 \cdot 10^{12}$	0.998
Produced at $T_r = 700$ °C	87.44	0.0919	$1.93 \cdot 10^{13}$	0.975
Produced at $T_r = 800$ °C	87.51	0.1139	$9.26 \cdot 10^{12}$	1.000

calculation of thermal parameters in Eq. (1) $\ln\left(\frac{Qf}{Rk}\right)$. As can be seen in Fig. 5, 5 of the 8 softwoods tested have similar slopes and ignition behaviour, namely feedstock and softwood produced at temperatures of 350 °C, 400 °C, 600 °C and 700 °C.

The thermal conductivity values of the softwood produced at the various reactor temperatures is one of the required physical parameters in this equation. Conductivity values were used for a temperature of 115 °C to ensure moisture effects were not encountered, as the self-heating experiments were carried out above 100 °C, but so that the value was in the range of experimental measurements carried out in the basket experiments. The values were therefore taken from Table 5 at 115 °C. By using these thermal conductivities and the value of the universal gas constant R , one can isolate the (Qf) , which is effectively a pre-exponential factor.

The results can therefore isolate all the thermal and kinetic parameters and a summary of all of these parameters is presented in Table 6, with R^2 calculated from the linear fit for each line. The error bounds are calculated using the fits that would give the highest and the lowest possible effective activation energy from the experimental data obtained (largest possible errors). The linear fits all have $R^2 > 0.975$, validating the Arrhenius reaction assumption.

4.2. Thermogravimetric analysis

Thermogravimetric analysis (TGA) was carried out in air with a heating rate of 10 K/min for all the softwood feedstock and biochar samples. The heating rate was chosen to have slow heating and therefore avoid thermal effects influencing experimental results. The reason for carrying out these measurements was to compare oxidative reactivity in microscale experiments so as to be able to have a link between the bulk scale experiments presented in this work and kinetics. Fig. 6 shows thermogravimetric analysis in air of the different softwood

biomasses and biochar measured in this work. All the samples display an initial reduction in mass due to drying of the softwood around 100 °C, then a large reduction in mass between 200 °C and 400 °C for the softwood feedstock, a less pronounced reduction in the same temperature range for biochar produced at pyrolysis temperatures of 350 °C and 400 °C, and then insignificant mass loss in the same temperature range for the biochar produced above 450 °C. This conforms to the theory section, where the hemicellulose and cellulose for biochars produced in a pyrolysis reactor above 450 °C are already reduced to a minimum and therefore the sample is made up of mostly lignin at this stage. All samples then present a steady mass loss above 400 °C. This can be further confirmed when analysing the mass loss rate of the samples calculated from the TGA of the biomasses several interesting trends can be clearly identified as seen in Fig. 7. Biochars produced above 450 °C all show reaction peaks at the same temperatures, with the only difference being the size of these mass loss peaks: the peak size decreases with increasing biochar pyrolysis temperature, and this can be explained by the fact that at high pyrolysis temperatures (600 °C and above) a lot of the lignin has pyrolysed [21], and we have less carbon present for oxidation reactions to take place. The characteristic temperatures where these mass losses occur are reported in Table 7, where it can be seen that for all the biochar apart from 350 °C the characteristic temperatures for mass loss and end of combustion increase with increasing pyrolysis temperature. When softwood is pyrolysed at very high temperatures, above 700 °C, the TGA curve does not plateau for the duration of the analysis.

5. Comparison to different biomass and biochar sources

Torrefied biomass and biochar can be produced at a variety of pyrolysis reactor temperatures from a variety of fuels. Section 4.1, has already shown that the pyrolysis reactor temperature is an important parameter when studying how prone softwood biochar is to self-heating ignition. However it has been shown in literature that the physiochemical properties of the products of pyrolysis reactors are not only dependent on reactor temperature, but also the starting organic material [35]. There is no current literature on the effect of torrefaction of biomass on self-heating ignition, and how that effect will change depending on the original feedstock material. We therefore additionally study the behavior of wheat pellets and rice husk feedstock and biochar produced at reactor temperatures of 450 °C, 550 °C and 700 °C to quantify the function of reactor temperature to propensity to self-heat for each of these starting organic materials and therefore compare the propensity of self-heating of the biomass and biochars produced from these different organic materials.

5.1. Material from varying feedstock

The biochars were produced from a wheat pellet feedstock, and rice husk feedstock pyrolysed in the same rotary kiln reactor used for the softwood [32], at 450 °C, 550 °C and 700 °C. The samples used in the experiments are presented in Fig. 8, and show different physical properties in terms of diameter, average length and bulk density of each. A summary of these characteristics is presented in Table 8 where the length range of pellets is presented in parenthesis. The rice husk samples were significantly smaller than the wheat pellets. Elemental analysis was carried out for all of the biochars and biomass feedstock to compare the CHN composition of each and is presented in Table 9. For wheat, the amount of carbon present in the char increases with increasing reactor temperature similarly to the results from softwood, which agrees with results in literature [33,36]. For rice husks, the amount of carbon decreases above the reactor temperature of 450 °C as more of the rice husk converts into oil, in agreement with what has been shown before in literature [37,38]. Both of these materials present less carbon than the softwood samples. Water, ash and Carbon in dry ash free basis (Cdaf) for the biomass and biochars are calculated using

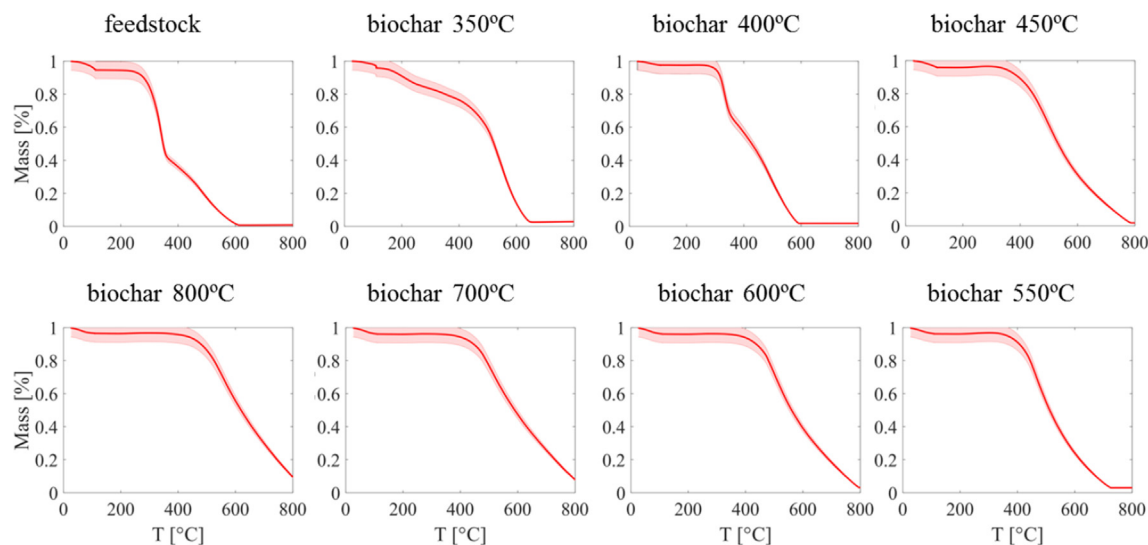


Fig. 6. Thermogravimetric analysis in air of the different softwood biomass and biochar samples carried out with a heating rate of 10 K/min. Each plot represents mass % as a function of temperature with error clouds taking into account experimental error.

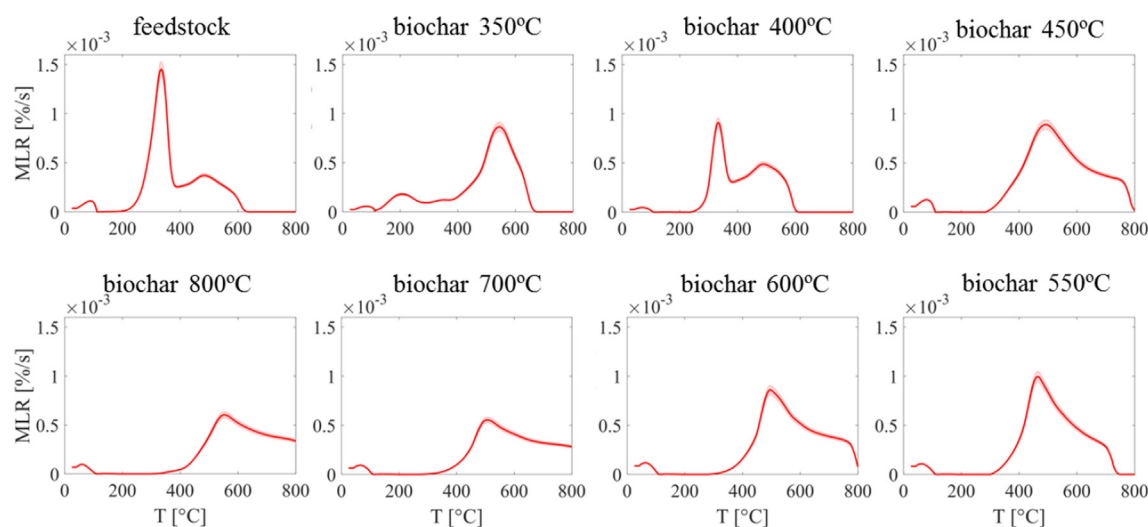


Fig. 7. Mass loss rates calculated from thermogravimetric analysis in air for softwood biomass and biochars samples. Each plot represents mass loss %/s as a function of temperature with error clouds taking into account experimental error.

Table 7

Characteristic temperatures for mass loss from Fig. 6.

Element	T characteristic 1 Temperature °C	T characteristic 2 Temperature °C
Softwood feedstock	260	600
Produced at $T_p = 350$ °C	120	650
Produced at $T_p = 400$ °C	300	690
Produced at $T_p = 450$ °C	330	790
Produced at $T_p = 550$ °C	350	725
Produced at $T_p = 600$ °C	350	795
Produced at $T_p = 700$ °C	350	810
Produced at $T_p = 800$ °C	380	815

the TGA data presented in 5.3 like for the softwood data. Results are presented in Table 10, where it can be seen that for rice husk the amount of Cdaf is significantly higher than the total carbon found in the elemental analysis, due to the high amount of ash produced in rice husk combustion. Furthermore, biochars pyrolysed at temperatures above 700 °C are purely carbon (apart from water and ash) for wheat (like for softwood previously), but not for rice husk.

Like for the softwood sample, the minimum critical ambient temperature for self-heating $T_{a,c}$ was determined experimentally. 82 experiments were carried out, with a summary of the experiments carried out presented in Table 11. In the same manner as for softwood, thermal conductivity properties were determined using a guarded heat flow meter for temperatures of 65 °C, 115 °C and 165 °C. Finally, to provide information on the reaction kinetics at the microscale of each pyrolysed biomass from the different feedstock sources, thermogravimetric analysis was conducted for each sample.

5.2. Basket experiments results for different biomass feedstock

For all the sample types, the minimum ignition temperature required for ignition was found for all three basket sizes. Fig. 9 shows the results of the basket experiments for the samples produced from wheat feedstock. As can be noted the lowest ignition temperature occurs for wheat biochar produced at a reactor temperature of 450 °C, like for the softwood samples in 4.1. Wheat biochar produced at reactor temperature of 550 °C is still more prone to self-heating ignition than the wheat feedstock, like for the biochar produced at reactor temperature of 700 °C which is less prone to self-heating ignition than the other

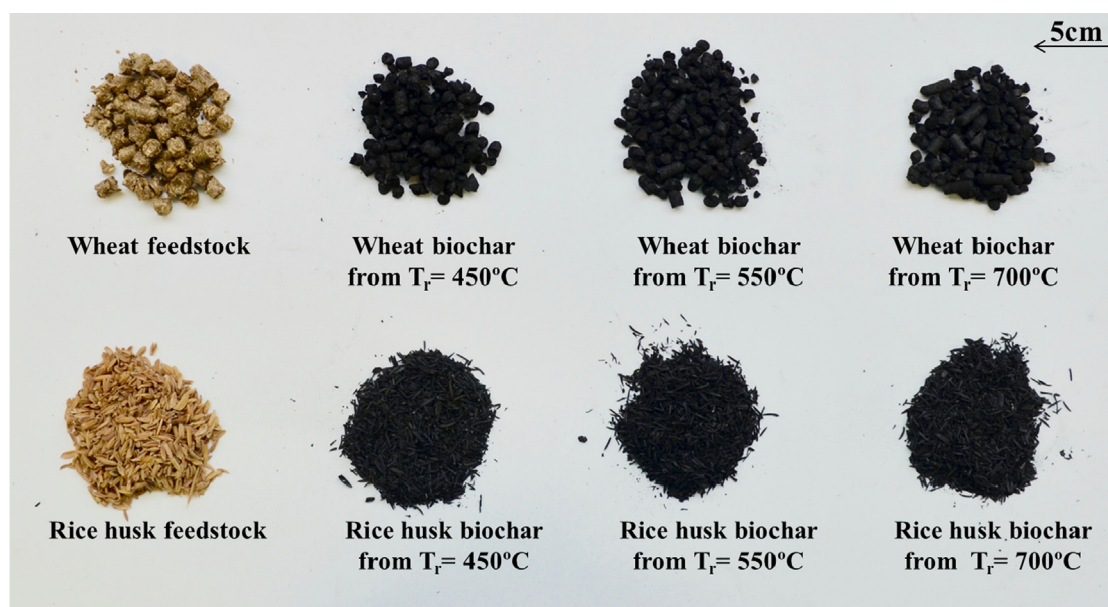


Fig. 8. Biomass and biochar samples used, with feedstock and various biochars produced in a pyrolysis reactors at temperatures of 450 °C, 550 °C, and 700 °C for wheat, and rice husk.

Table 8

Physical properties of wheat and rice husk biomass and biochar used for experiments.

Physical properties	Density (kg/m ³)	Pellet length (mm)	Pellet diameter (mm)
Wheat feedstock	389	15 (12,18)	6.5
Wheat biochar produced at $T_r = 450$ °C	215	11 (9,13)	5.0
Wheat biochar produced at $T_r = 550$ °C	204	11 (9,13)	4.8
Wheat biochar produced at $T_r = 700$ °C	255	10 (8,12)	4.6
Rice husk feedstock	110	8	1.6
Rice husk biochar produced at $T_r = 450$ °C	82	5	0.4
Rice husk biochar produced at $T_r = 550$ °C	77	5	0.6
Rice husk biochar produced at $T_r = 700$ °C	95	5	0.4

Table 9

Elemental analysis of the wheat and rice biomass and biochars.

Element	C Weight %	H	N
Wheat feedstock	42.7	6.2	0.4
Wheat biochar produced at $T_r = 450$ °C	60.0	3.2	1.3
Wheat biochar produced at $T_r = 550$ °C	68.4	2.8	0.8
Wheat biochar produced at $T_r = 700$ °C	77.4	2.2	< 0.3
Rice husk feedstock	36.5	5.2	< 0.3
Rice husk biochar produced at $T_r = 450$ °C	48.9	2.6	0.52
Rice husk biochar produced at $T_r = 550$ °C	47.0	2.0	< 0.3
Rice husk biochar produced at $T_r = 700$ °C	41.5	1.3	< 0.3

biochars but still more than the feedstock.

Similarly, Fig. 10 shows the results of the basket experiments for the samples produced from rice husk feedstock. The lowest ignition temperature occurs for rice biochar produced at a reactor temperature of 450 °C, like for both the softwood and the wheat samples. Rice biochar produced at a reactor temperature of 550 °C is less prone to self-heating ignition than the rice feedstock, which is a different behaviour with respect to the wheat and softwood equivalents. The biochar produced at

reactor temperature of 700 °C is the least prone to self-heating. The rice products are generally less prone to self-heating, resulting in higher minimum ignition temperatures for same sized boxes and same reactor temperatures when compared to both the softwood and wheat products. For the 10.16 cm length cube box, the difference in ignition temperature for the rice and softwood biochar produced at 450 °C is over 40 °C, making the self-heating ignition behaviour of the biochar produced from different biomass materials significantly different.

Plotting the minimum ignition temperature for one basket size (10.16 cm length basket) for all the biochars with respect to the carbon dry free ash allows a comparison of the effect of total carbon content with the critical ignition temperature. This has already been done for the softwood in Section 4.1, and is done for wheat in Fig. 11 and rice husk in Fig. 12. The results for wheat show that the peak at 450 °C is not solely caused by the carbon content, as the V shape seen in Fig. 9 is also clearly present in this plot, and behaves very similarly to the softwood. The rice husks have a slightly different behaviour, as the carbon content of rice husk produced at pyrolysis temperatures of 550 °C has a higher carbon dry ash free content than the one produced at 700 °C, causing the shape not to follow the same V shape as the previous two materials. However the trend of a local minimum at 450 °C production temperature is still found for rice husk.

Conductivity was measured experimentally using the guarded heat flow meter method at various temperatures, and was shown to be linear within our measured temperature range between 65 and 165 °C for all biomass products, irrespective of the biomass used. A summary of the conductivity measurements is presented in Table 12. Some patterns were found in the conductivity properties: like seen earlier in softwood, for wheat the most conductive of material was the feedstock, with the biochar produced at 450 °C the least conductive and biochars produced at higher reactor temperatures increasing in thermal conductivity, but staying below the thermal conductivity of the feedstock. Between wheat and softwood, wheat is slightly more conductive. The fact that the biochar was produced at 450 °C contributes to why the biochar produced at this temperature is the most prone to ignite, as the exothermic reactions at the core of the sample cannot be as effectively cooled by the ambient temperature due to the fact that the surrounding biochar acts as a good insulator. On the other hand, for rice husk the thermal conductivity behaviour observed from the experiments is different, as the least conductive of the samples is the rice feedstock, with increasing

Table 10

Water, ash and Carbon in dry ash free basis (Cdaf) for the biomass and biochars calculated using the TGA data presented in Section 5.3.

Element	Water weight %	Ash	Cdaf
Wheat feedstock	4.6	4.9	47.1
Wheat biochar produced at $T_r = 450^\circ\text{C}$	4.5	19.5	78.9
Wheat biochar produced at $T_r = 550^\circ\text{C}$	3.3	20.8	90.1
Wheat biochar produced at $T_r = 700^\circ\text{C}$	3.4	18.7	99.5
Rice husk feedstock	3.7	21.0	48.5
Rice husk biochar produced at $T_r = 450^\circ\text{C}$	3.6	39.9	86.5
Rice husk biochar produced at $T_r = 550^\circ\text{C}$	2.6	47.5	94.1
Rice husk biochar produced at $T_r = 700^\circ\text{C}$	2.3	49.4	86.0

Table 11

Number of experiments carried out for each type of biomass and biochar, ordered on the basis of feedstock type and basket sizes.

Pellet type	Basket length (cm)		
	5.1	7.6	10.2
Wheat feedstock	4	3	2
Wheat biochar produced at $T_r = 450^\circ\text{C}$	6	3	2
Wheat biochar produced at $T_r = 550^\circ\text{C}$	4	3	3
Wheat biochar produced at $T_r = 700^\circ\text{C}$	2	3	3
Rice husk Feedstock	7	3	2
Rice husk biochar produced at $T_r = 450^\circ\text{C}$	4	3	2
Rice husk biochar produced at $T_r = 550^\circ\text{C}$	6	3	2
Rice husk biochar produced at $T_r = 700^\circ\text{C}$	6	3	3

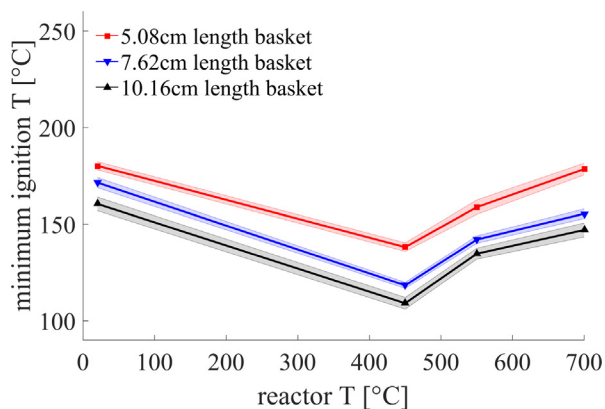


Fig. 9. Minimum ignition temperature for wheat feedstock and biochar produced at 450°C , 550°C , and 700°C for three basket sizes. Experimental error is estimated based on temperature error bounds on each individual set of experiments.

thermal conductivity with respect to increasing reactor temperature.

Using the experimental results from the basket experiments and the Frank-Kamenetskii theory of criticality we extract a one-step kinetic model and thermal parameters by plotting $\ln(\delta_c T_{a,c}/L^2)$ vs $1/T_{a,c}$ like done for softwood, and the results are shown in Fig. 13 for wheat and Fig. 14 for rice. A few observations from these plots, compared to the previous results for softwood, are that for both softwood, wheat, and rice husks the characteristics of the slopes of the feedstock and biochar produced at reactor temperatures of 700°C are quite similar. Using the thermal conductivity data presented in Table 12, we then isolate all the thermal and kinetic parameters and a summary of all of these parameters is presented in Table 13, with R^2 calculated from the linear fit for each line. The error bounds are calculated using the fits that would give the highest and the lowest possible effective activation energy from the experimental data obtained (largest possible errors).

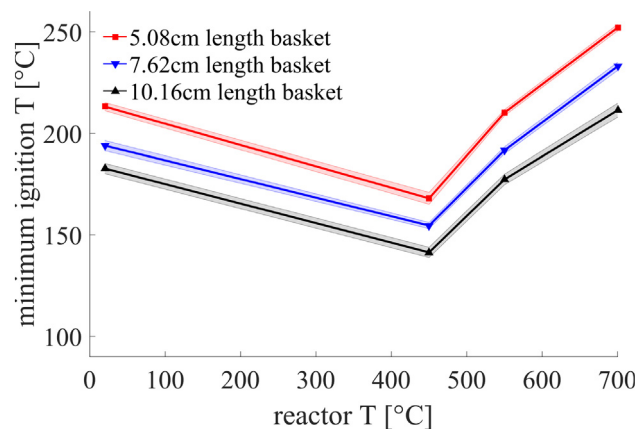


Fig. 10. Minimum ignition temperature for rice husk feedstock and biochar produced at 450°C , 550°C , and 700°C for three basket sizes. Experimental error is estimated based on temperature error bounds on each individual set of experiments.

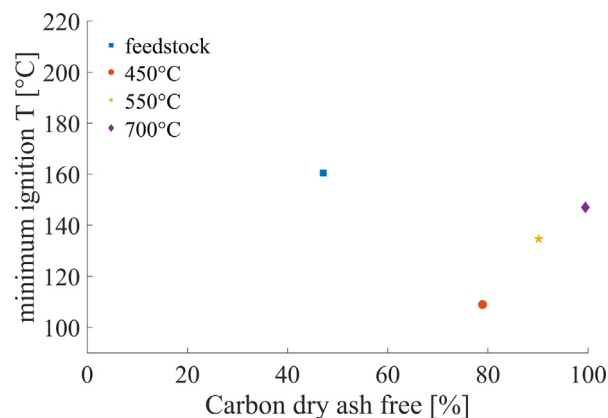


Fig. 11. Minimum ignition temperature for wheat feedstock and biochar between 450°C and 700°C for a fixed basket size plotted vs carbon dry ash free.

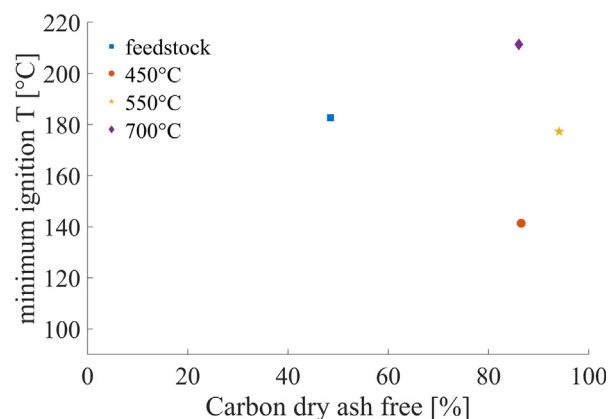


Fig. 12. Minimum ignition temperature for rice husk feedstock and biochar between 450°C and 700°C for a fixed basket size plotted vs carbon dry ash free.

5.3. Thermogravimetric analysis from various feedstock

Like for softwood, to link these bulk scale self-heating basket experiments to the oxidative reactivity carried out in microscale experiments, TGA was carried out in air with a heating rate of 10 K/min for all the feedstock and biochar samples. Fig. 15 shows the results of the mass loss found in each sample from TGA. All the samples display an initial reduction in mass due to drying of the sample around 100°C , then a

Table 12

Thermal conductivity measurements for the biomass samples conducted at 3 temperatures, with resulting fit equation. The R^2 values of the linear fits through these points are included.

k for biomass type	65 °C (W/mK)	115 °C (W/mK)	165 °C (W/mK)	R^2 (–)
Wheat feedstock	0.1397	0.1502	0.1715	0.963
Wheat biochar produced at $T_r = 450$ °C	0.0881	0.0908	0.0980	0.935
Wheat biochar produced at $T_r = 550$ °C	0.0879	0.0977	0.1061	0.998
Wheat biochar produced at $T_r = 700$ °C	0.1082	0.1186	0.1243	0.971
Rice husk feedstock	0.1055	0.1129	0.1239	0.990
Rice husk biochar produced at $T_r = 450$ °C	0.1256	0.1360	0.1424	0.981
Rice husk biochar produced at $T_r = 550$ °C	0.1266	0.1469	0.1588	0.977
Rice husk biochar produced at $T_r = 700$ °C	0.1222	0.1350	0.1469	1.000

Table 13

Effective activation energy E , pre-exponential factor Q_f , conductivity k extracted from Frank-Kamenetskii plot (Figs. 13–14 calculated using Eq. (2)). The R^2 values of the linear fits used to calculate these are included.

Biomass type	E (kJ/mol)	k (W/mK)	Q_f (W/m ³)	R^2 (–)
Wheat feedstock	120.68	0.1502	$6.22 \cdot 10^{17}$	0.972
Wheat biochar produced at $T_r = 450$ °C	67.76	0.0908	$3.06 \cdot 10^{12}$	0.994
Wheat biochar produced at $T_r = 550$ °C	92.20	0.0977	$4.21 \cdot 10^{14}$	0.989
Wheat biochar produced at $T_r = 700$ °C	74.09	0.1186	$4.08 \cdot 10^{12}$	0.982
Rice husk feedstock	91.20	0.1129	$6.02 \cdot 10^{13}$	0.999
Rice husk biochar produced at $T_r = 450$ °C	86.18	0.1360	$1.53 \cdot 10^{14}$	0.989
Rice husk biochar produced at $T_r = 550$ °C	84.17	0.1469	$1.63 \cdot 10^{13}$	0.998
Rice husk biochar produced at $T_r = 700$ °C	79.75	0.1350	$1.21 \cdot 10^{12}$	0.980

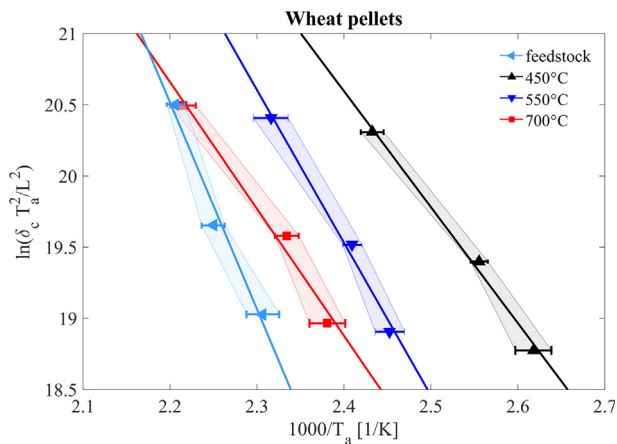


Fig. 13. Frank-Kamenetskii plot for wheat feedstock and biochar produced at 450 °C, 550 °C, and 700 °C. Experimental error is estimated based on error bounds on each individual set of experiments. The linear fits all have $R^2 > 0.972$ (Table 13).

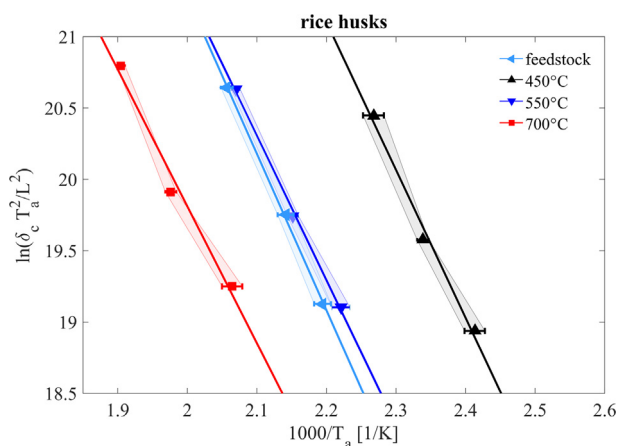


Fig. 14. Frank-Kamenetskii plot for rice husk feedstock and biochar produced at 450 °C, 550 °C, and 700 °C. Experimental error is estimated based on error bounds on each individual set of experiments. The linear fits all have $R^2 > 0.982$ (Table 13).

large reduction in mass between 200 °C and 400 °C. Mass loss continues until 600 °C for all the samples. Differences can be seen in the mass loss of the different materials: rice husk has a significantly higher residue than wheat (and softwood results from previous section). For rice husk feedstock the residue is just over 20% of the initial mass, while for wheat feedstock around 5%. This significant difference in residue is also

found for the biochars, where for rice biochars the residue mass ranges from 40% to 50% of the original mass, compared to wheat biochar which has around 20% residue mass and softwood biochar from previous section which was found to have negligible residue. The characteristic temperatures where these mass losses occur are reported in Table 14, where it can be seen that for all the materials both the first and second characteristic temperature increase with increasing pyrolysis temperature.

Analysing the mass loss rate (MLR) of the samples calculated from the TGA of the biomasses, several trends can be clearly identified and are presented in Fig. 16. Both feedstocks present two peaks around 350 °C and 450 °C the first corresponding to a large loss of hemicellulose and cellulose, the second to a loss of lignin [21]. The biochars do not present these two peaks, as they are all produced at reactor temperatures above 450 °C, therefore past the decomposition of the hemicellulose and cellulose. Therefore one peak is seen, decomposition of the lignin [21]. This is the same as found for softwood in Section 4.2. For the rice husk all biochars show peaks of mass loss rates at the same temperature, around 550 °C, and of the same magnitude. The wheat biochar shows similarly sized peaks but at a slightly lower temperature just above 400 °C. For all the biochars, the magnitude of the MLR tends to decrease with increasing biochar pyrolysis temperature, and this can be explained by the fact that at high pyrolysis temperatures (600 °C and above) a lot of the lignin has already pyrolysed [21], and we have less carbon present for oxidation reactions to take place.

6. Upscaling of results

The results presented in this work can be used together with Frank-Kamenetskii theory to upscale the laboratory results to large biomass and biochar stockpiles of cubic size. Some examples of such systems are standard domestic biomass storage units (10 m³) or open top container trucks (30 m³) for transport. The upscaled results are presented in Fig. 17 for a temperature range from –10 °C to 40 °C for softwood feedstock and softwood biochar produced at pyrolysis reactor temperatures between 350 °C and 800 °C. The temperature range of upscaling was chosen to span the range of ambient temperatures expected in power plants. Some significant results from this figure are that softwood biochar pellets produced at 450 °C of the dimensions of even a standard domestic biomass storage unit (2.2 m cube height) will ignite from self-heating at ambient temperatures as low as 20 °C. On the other hand biochar produced at high pyrolysis reactor temperatures like 800 °C would not ignite from self-heating in containers of the same size even for temperatures of 70 °C. Softwood feedstock is similarly safe for handling when stored in spaces smaller than 8000 m³ for temperatures below 40 °C. This shows that for biochar transport storage and handling the production mechanism is very important, as there is large variation

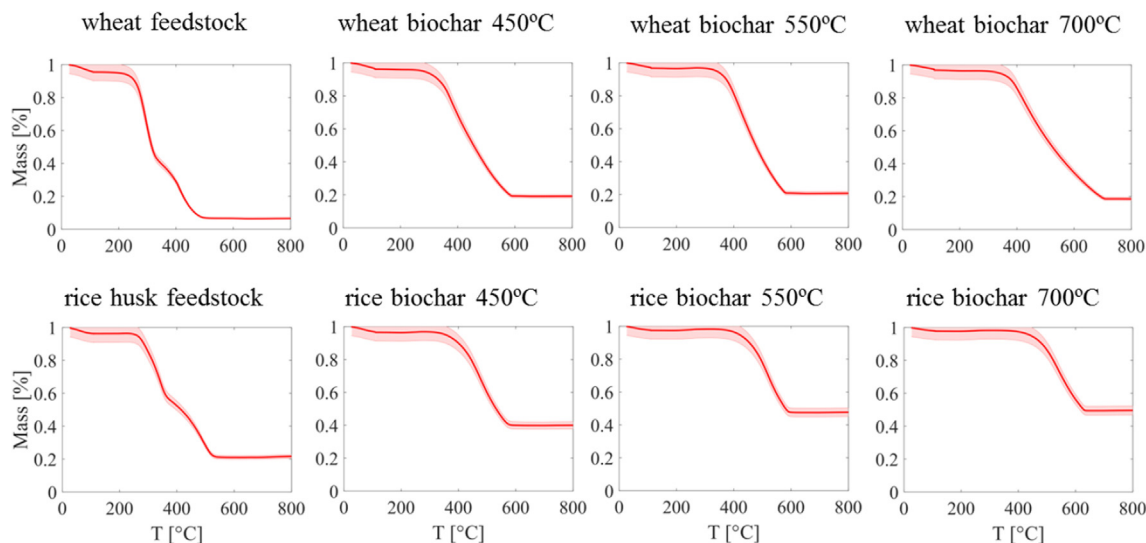


Fig. 15. Thermogravimetric analysis in air of the wheat and rice husk biomass and biochar samples carried out with a heating rate of 10 K/min. Each plot represents mass % as a function of temperature with error clouds taking into account experimental error.

Table 14

Characteristic temperatures for mass loss from Fig. 15.

Element	T characteristic 1 Temperature °C	T characteristic 2 Temperature °C
Wheat feedstock	200	500
Wheat biochar produced at $T_r = 450^\circ\text{C}$	270	680
Wheat biochar produced at $T_r = 550^\circ\text{C}$	310	580
Wheat biochar produced at $T_r = 700^\circ\text{C}$	320	700
Rice husk feedstock	240	550
Rice husk biochar produced at $T_r = 450^\circ\text{C}$	300	600
Rice husk biochar produced at $T_r = 550^\circ\text{C}$	350	600
Rice husk biochar produced at $T_r = 700^\circ\text{C}$	400	630

in the biochar's propensity to self-ignite. As shown experimentally softwood biochar produced at 450°C is the most prone to self-heating ignition, even for relatively modest storage sizes of (10 m^3), and therefore particular care must be taken when transporting and storing said softwood. The upscaling requires oxidizer to be present for the

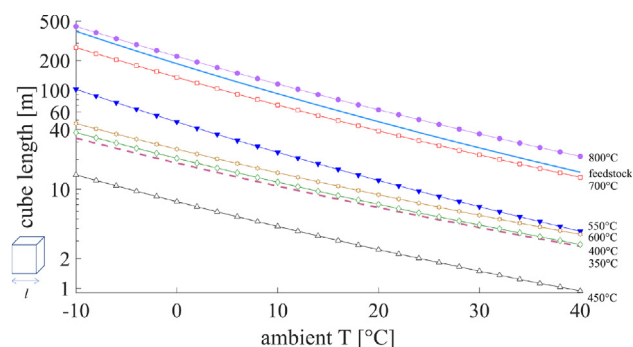


Fig. 17. Upscaled results of cubic biomass and biochar piles required for self-ignition for ambient temperature between -10°C and 40°C based on the thermal and kinetic parameters found in self-heating basket experiments (Table 6).

reactions to take place, but in the example of domestic storage or open-top truck transport, oxygen is readily available.

When upscaling results for the wheat biochar, shown in Fig. 18, we

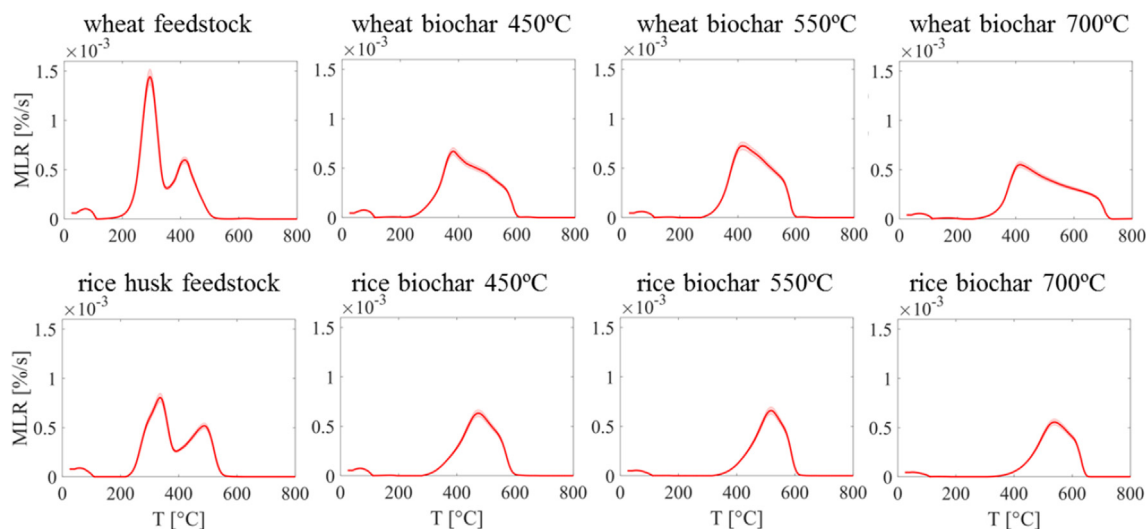


Fig. 16. Mass loss rates calculated from thermogravimetric analysis in air for the wheat and rice husk biomass and biochars samples. Each plot represents mass loss %/s as a function of temperature with error clouds taking into account experimental error.

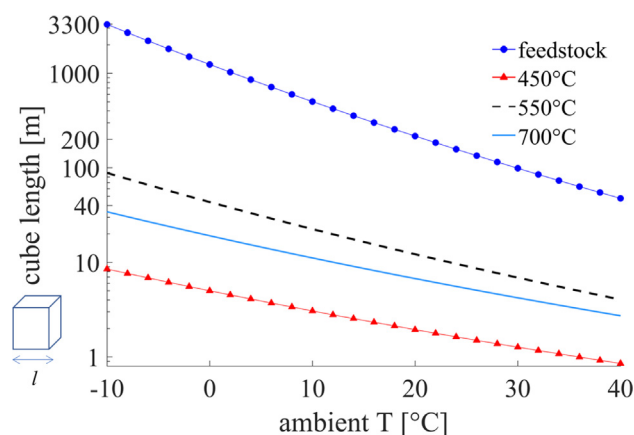


Fig. 18. Upscaled results of cubic wheat biomass and biochar piles required for self-ignition at ambient temperature between -10°C and 40°C based on the thermal and kinetic parameters found in self-heating basket experiments (Table 13).

see a similar ignition trend to that of softwood for the biochar pellets produced at 450°C . For a sample of the dimensions of even a standard domestic biomass storage unit (2.2 m cube height) will ignite from self-heating at ambient temperatures as low as 16°C . Biochar produced at a reactor temperature of 550°C would not ignite from self-heating in a container of the same size, nor an open top container for temperatures up to 40°C . Similarly, feedstock would require a much larger critical size to ignite at temperatures below 40°C . However, and quite differently than the result found for softwood, wheat biochar produced at 700°C would be at risk of self-heating ignition in volumes the size of open top containers for temperatures around 38°C .

The upscaling of the rice husk pile sizes (Fig. 19) shows that for all analysed samples, i.e. rice husk feedstock and biochar produced at reactor temperatures of 450°C , 550°C and 700°C the required size for self-heating ignition is well above the threshold of both domestic size storage units and open top containers in the temperature range between -10°C and 40°C , meaning these samples are less prone to self-heating ignition in these typical environmental conditions and sizes with respect to both the softwood and wheat biomass and biochars.

7. Discussion

In this paper, bench-scale experiments were conducted to determine the effect of pyrolysis reactor temperature used in the production of biochar on the propensity to ignite for self-heating for that given

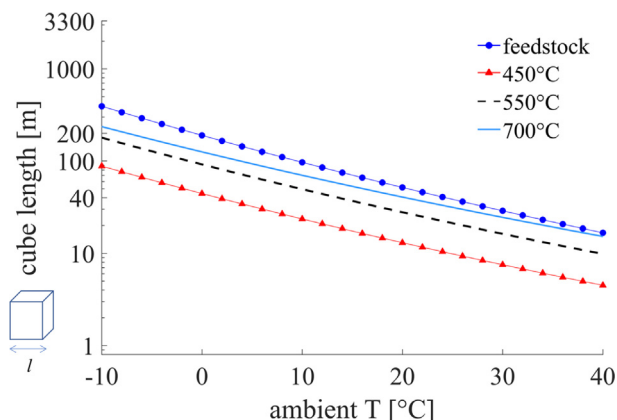


Fig. 19. Upscaled results of cubic rice husk biomass and biochar piles required for self-ignition at ambient temperature between -10°C and 40°C based on the thermal and kinetic parameters found in self-heating basket experiments (Table 13).

material. Softwood was pyrolysed at seven different pyrolysis reactor temperatures and basket experiments, thermogravimetric analysis and physical parameter measurements were carried out for each biochar product as well as the original softwood feedstock. Self-heating basket experiments quantified the ignition temperature for 3 given critical volumes for self-ignition criteria for the biochars. The results show that the reactivity of the softwood is not a monotonic function of pyrolysis reactor temperature. In fact, results show that biochar produced at a reactor temperature of 450°C is the most prone to self-heating, and that the reactivity of the softwood increases with reactor temperature up to 450°C but then significantly decreases, and for reactor temperatures above 550°C , the softwood is less reactive than the feedstock. Using the Frank-Kamenetskii theory to extract thermal and kinetic parameters, effective activation energies with pre-exponential factors were determined for each biochar sample and were summarised in Table 6. Results showed that for reactor temperatures above 600°C the biochar was less prone to self-heating than the original softwood feedstock. Thermal conductivity measurements of the different biochars also show that the least conductive of the softwoods is the one produced at reactor temperature of 450°C , which can contribute to the increased proneness to self-heating ignition as the biochar acts as a more efficient insulator compared to the other biochars tested, while the feedstock softwood being the most conductive.

However different feedstock sources showed different proneness to self-heating ignition. By additionally testing wheat pellets and rice husks feedstock and respective biochars produced at three pyrolysis temperatures we showed from the experimental laboratory bench-scale studies that the material most prone to self-heating ignition was softwood, but softwood and wheat showed very similar characteristics. The rice husk was shown to be overall less prone to self-heating ignition, with an upscaling analysis showing that at typical temperature ranges found in areas like power plant storage the required pile size of rice husk or one of its biochar products is well above what is found in standard domestic storage or open-top transport containers. In total, 173 experiments were carried out with 1036 h of oven run time for studying all three types of feedstock.

The different biochars present in this work have different physical properties, as reported in Tables 2, 3, 5, 9, 10, and 12. Therefore it is hard to quantify the overall effect of devolatilization, porosity of the char and condensed volatiles individually on the effect of self-heating ignition. Work by Masek et al. [32] aims to quantify char yield, and volatile matter content with different pyrolysis temperatures, and finds that increasing pyrolysis temperature reduces volatile matter content in the biochars. However to the authors' knowledge effect of pore size has not yet been explored, and could be relevant for future work.

The bench-scale experiments were extended to large-scale systems to compare to real storage and transport sizes using the experimentally measured effective activation energies and thermal parameters. This shows that both wheat and softwood biochar produced at pyrolysis reactor temperatures of 450°C are prone to self-heating ignition at ambient temperatures as low as 16°C and 20°C respectively, for dimensions as small as domestic biomass storage sizes, making it a fire hazard. This paper is the first in-depth experimental quantification of self-heating ignition of biomass and biochar as a function of pyrolysis reactor temperature used for production and feedstock origin, giving kinetic and thermal parameters that can be used to calculate safe sizes for transport and storage of biomass and biochars. The work shows that it is very important to know at what conditions biochar is produced as its proneness to self-heating ignition varies dramatically with biochar production temperature and can vary based on feedstock material.

8. Conclusions

Softwood pyrolysed at seven different pyrolysis reactor temperatures was used in basket experiments, thermogravimetric analysis and physical parameter measurements including thermal conductivities to

quantify for the first time in literature how self-heating ignition and pyrolysis reactor temperature are related. The results show that the reactivity of the softwood is not a monotonic function of pyrolysis reactor temperature, with a peak in reactivity for biochar produced at a reactor temperature of 450 °C, and a sharp decrease in reactivity for biochar produced at temperatures over 100 °C away from 450 °C. Wheat and rice husk biomass and biochars were also tested to compare different source feedstock effects on self-heating ignition properties. This paper quantifies kinetic and thermal parameters that can be used to calculate safe sizes for transport and storage of different biomass and biochars.

Acknowledgements

This research was funded by EPSRC (grant EP/L504786/1). The authors would like to thank Franz Richter and Nieves Fernandez-Anez (Imperial College London) for valuable discussions. Data supporting this publication can be obtained from <https://zenodo.org/communities/imperialhazlab/> under a Creative Commons Attribution license.

References

- [1] Parikka M. Global biomass fuel resources. *Biomass Bioenergy* 2004;27(6):613–20. <https://doi.org/10.1016/j.biombioe.2003.07.005>.
- [2] De S, Assadi M. Impact of cofiring biomass with coal in power plants – A techno-economic assessment. *Biomass Bioenergy* 2009;33(2):283–93. <https://doi.org/10.1016/j.biombioe.2008.07.005>.
- [3] Van der Stelt M, Gerhauser H, Kiel J, Ptasiński K. Biomass upgrading by torrefaction for the production of biofuels: a review. *Biomass Bioenergy* 2011;35(9):3748–62.
- [4] Dullien FAL. Porous media: fluid transport and pore structure. Academic Press; 1979.
- [5] Ohlemiller TJ. Smouldering combustion. *SFPE Handbook Fire Protection Eng* 1995:171–9.
- [6] Bowes P. Self-heating: evaluating and controlling the hazards. London: HMSO; 1984.
- [7] Drysdale D. An introduction to fire dynamics. 3rd ed. Chichester: Wiley and Sons; 2011. <https://doi.org/10.1002/9781119975465>.
- [8] Brinton WF, Droffner ML, Brinton RB. A standardized dewar test for evaluation of compost self-heating. *Biocycle Rep* 1982;1995:1–16.
- [9] Semenov NN. Chain reactions [Goskhimizdat]. [English translation]. Oxford; 1935.
- [10] Babrauskas V. Ignition handbook. Fire Science Publishers; 2003.
- [11] Restuccia F, Huang X, Rein G. Self-ignition of natural fuels: can wildfires of carbon-rich soil start by self-heating? *Fire Safety J* 2017;91(Supplement C):828–34. <https://doi.org/10.1016/j.firesaf.2017.03.052>. fire Safety Science: Proceedings of the 12th International Symposium.
- [12] Restuccia F, Ptak N, Rein G. Self-heating behavior and ignition of shale rock. *Combust Flame* 2017;176:213–9. <https://doi.org/10.1016/j.combustflame.2016.09.025>.
- [13] Stott P. Combustion in tropical biomass fires: a critical review. *Prog Phys Geogr* 2000;24(3):355–77.
- [14] Grotkjær T, Dam-Johansen K, Jensen AD, Glarborg P. An experimental study of biomass ignition. *Fuel* 2003;82(7):825–33. [https://doi.org/10.1016/S0016-2361\(02\)00369-1](https://doi.org/10.1016/S0016-2361(02)00369-1).
- [15] García-Torrent J, Ramírez-Gómez A, Querol-Aragón E, Grima-Olmedo C, Medić-Pejić L. Determination of the risk of self-ignition of coals and biomass materials. *J Hazard Mater* 2012;213–214:230–5. <https://doi.org/10.1016/j.jhazmat.2012.01.086>.
- [16] Bilbao R, Mastral JF, Aldea ME, Ceamanos J, Betrán M, Lana JA. Experimental and theoretical study of the ignition and smoldering of wood including convective effects. *Combust Flame* 2001;126(1–2):1363–72. [https://doi.org/10.1016/S0016-2180\(01\)00251-6](https://doi.org/10.1016/S0016-2180(01)00251-6).
- [17] Van Blijdervheen M, Bramer EA, Brem G. Modelling spontaneous ignition of wood, char and RDF in a lab-scale packed bed. *Fuel* 2013;108(9):190–6. <https://doi.org/10.1016/j.fuel.2010.01.021>.
- [18] García-Torrent J, Fernandez Anez N, Medić-Pejić L, Montenegro Mateos L. Assessment of self-ignition risks of solid biofuels by thermal analysis. *Fuel* 2015;143:484–91. <https://doi.org/10.1016/j.fuel.2014.11.074>.
- [19] Jones JM, Saddawi A, Dooley B, Mitchell EJS, Werner J, Waldron DJ, et al. Low temperature ignition of biomass. *Fuel Process Technol* 2015;134:372–7. <https://doi.org/10.1016/j.fuproc.2015.02.019>.
- [20] Fernandez Anez N, García-Torrent J, Medić-Pejić L, Grima Olmedo C. Detection of incipient self-ignition process in solid fuels through gas emissions methodology. *J Loss Prev Process Ind* 2015;36:343–51. <https://doi.org/10.1016/j.jlpp.2015.02.010>.
- [21] Yang H, Yan R, Chen H, Zheng C, Lee DH, Liang DT. In-depth investigation of biomass pyrolysis based on three major components: hemicellulose, cellulose and lignin. *Energy Fuels* 2006;20(17):388–93. <https://doi.org/10.1021/ie1025453>.
- [22] Raveendran K, Ganesh A, Khilar KC. Pyrolysis characteristics of biomass and biomass components. *Fuel* 1996;75(8):987–98. [https://doi.org/10.1016/0016-2361\(96\)00030-0](https://doi.org/10.1016/0016-2361(96)00030-0).
- [23] Downie A, Munroe P, Crosky A. Characteristics of biochar- physical and structural properties. In: Lehmann J, Joseph S, editors. *Biochar for environmental management: science and technology*; 2009. p. 13–29 [Chapter 2].
- [24] Juita, Dlugogorski BZ, Kennedy EM, Mackie JC. Low temperature oxidation of linseed oil: a review. *Fire Sci Rev* 2012;1(1):3. <https://doi.org/10.1186/2193-0414-1-3>.
- [25] Worden JT. Spontaneous ignition of linseed oil soaked cotton using the oven basket and crossing point methods. Maryland: University of Maryland; 2011.
- [26] Gray B. In: *SFPE handbook of fire protection engineering*, 4th ed.; 2008. Ch. 2–10: spontaneous combustion and self-heating. p. 241–58.
- [27] Nelson MI, Marchant TR, Wake GC, Balakrishnan E, Chen XD. Self-heating in compost piles due to biological effects. *Chem Eng Sci* 2007;62(17):4612–9. <https://doi.org/10.1016/j.ces.2007.05.018>.
- [28] Hogland W, Marques M. Physical, biological and chemical processes during storage and spontaneous combustion of waste fuel. *Resour Conserv Recycl* 2003;40(1):53–69. [https://doi.org/10.1016/S0921-3449\(03\)00025-9](https://doi.org/10.1016/S0921-3449(03)00025-9).
- [29] Yang YB, Sharifi VN, Swithenbank J. Effect of air flow rate and fuel moisture on the burning behaviours of biomass and simulated municipal solid wastes in packed beds. *Fuel* 2004;83(11–12):1553–62. <https://doi.org/10.1016/j.fuel.2004.01.016>.
- [30] Beamish BBT, Hamilton GR. Effect of moisture content on the R 70 self-heating rate of Cillide coal. *Int J Coal Geol* 2005;64:133–8. <https://doi.org/10.1016/j.jcoal.2005.03.011>.
- [31] Clemens AH, Matheson TW. The role of moisture in the self-heating of low-rank coals. *Fuel* 1996;75(7):891–5. [https://doi.org/10.1016/0016-2361\(96\)00010-5](https://doi.org/10.1016/0016-2361(96)00010-5).
- [32] Mašek O, Buss W, Roy-Poirier A, Lowe W, Peters C, Brownsort P, et al. Consistency of biochar properties over time and production scales: a characterisation of standard materials. *J Anal Appl Pyrol* 2018;132:200–10. <https://doi.org/10.1016/j.jaap.2018.02.020>.
- [33] Mašek O, Brownsort P, Cross A, Sohi S. Influence of production conditions on the yield and environmental stability of biochar. *Fuel* 2013;103:151–5. <https://doi.org/10.1016/j.fuel.2011.08.044>.
- [34] BSI. BS EN 15296:2011 Solid biofuels. Conversion of analytical results from one basis to another; 2011.
- [35] Enders A, Hanley K, Whitman T, Joseph S, Lehmann J. Characterization of biochars to evaluate recalcitrance and agronomic performance. *Bioresour Technol* 2012;114:644–53. <https://doi.org/10.1016/j.biortech.2012.03.022>.
- [36] Zhao L, Cao X, Mašek O, Zimmerman A. Heterogeneity of biochar properties as a function of feedstock sources and production temperatures. *J Hazard Mater* 2013;256–257:1–9. <https://doi.org/10.1016/j.jhazmat.2013.04.015>.
- [37] Maiti S, Dey S, Purakayastha S, Ghosh B. Physical and thermochemical characterization of rice husk char as a potential biomass energy source. *Bioresour Technol* 2006;97(16):2065–70. <https://doi.org/10.1016/j.biortech.2005.10.005>.
- [38] Tsai WT, Lee MK, Chang YM. Fast pyrolysis of rice husk: product yields and compositions. *Bioresour Technol* 2007;98(1):22–8. <https://doi.org/10.1016/j.biortech.2005.12.005>.